Biol. Cybern. 49, 155-167 (1984)

Biological Cybernetics

The Interspike Interval of a Cable Model Neuron with White Noise Input

Henry C. Tuckwell[1], Frederic Y. M. Wan[2], and Yau Shu Wong[3]

1 Department of Mathematics, Monash University, Clayton, Victoria, Australia
2 Department of Mathematics, and Institute of Applied Mathematics and Statistics, University of British Columbia, Vancouver, Canada
3 Department of Mathematics, McGill University, Burnside Hall, Montreal, Quebec, Canada

Abstract. The firing time of a cable model neuron in response to white noise current injection is investigated with various methods. The Fourier decomposition of the depolarization leads to partial differential equations for the moments of the firing time. These are solved by perturbation and numerical methods, and the results obtained are in excellent agreement with those obtained by Monte Carlo simulation. The convergence of the random Fourier series is found to be very slow for small times so that when the firing time is small it is more efficient to simulate the solution of the stochastic cable equation directly using the two different representations of the Green's function, one which converges rapidly for small times and the other which converges rapidly for large times. The shape of the interspike interval density is found to depend strongly on input position. The various shapes obtained for different input positions resemble those for real neurons. The coefficient of variation of the interspike interval decreases monotonically as the distance between the input and trigger zone increases. A diffusion approximation for a nerve cell receiving Poisson input is considered and input/output frequency relations obtained for different input sites. The cases of multiple trigger zones and multiple input sites are briefly discussed.

1 Introduction

Previous theoretical investigations of the responses of nerve cells which receive random inputs have treated a cell as a point object characterized by a single membrane potential. When this membrane potential reaches some assigned threshold, the neuron is assumed to fire an action potential and the time between action potentials is referred to as the interspike interval. There have been many attempts to determine the statistical properties of the interspike interval (Stein, 1965, 1967; Gluss, 1967; Roy and Smith, 1969; Capocelli and Ricciardi, 1971; Tuckwell, 1975 ; White and Ellias, 1977; Cope and Tuckwell, 1980; Wilbur and Rinzel, 1983 ; Wan and Tuckwell, 1982; Vasudevan and Vittal, 1982; Hanson and Tuckwell, 1983) employing a variety of such point models. All these one-dimensional models suffer from the deficiency of ignoring the fact that nerve cells have considerable spatial extent and that the random inputs may occur almost anywhere on the soma-dendritic surface.

In deterministic neural modelling, the spatial extent of the cell has been taken into account. For subthreshold depolarization the cable model has been employed with considerable success since its first confirmation by Hodgkin and Rushton (1946) for certain kinds of axon. The importance of the dendritic contribution to the integration of inputs and the response to current injections was first investigated by Rall (1957, 1959, 1960). In these theoretical studies the membrane potential was assumed to be governed by the linear cable equation, which can be written in the form

$$V_t = -V + V_{xx} + kI, \quad 0 < x < L, \quad t > 0, \tag{1.1}$$

where V is the depolarization in volts, x and t are dimensionless space and time variables, $I(x,t)$ is the input current density and k is a parameter associated with a particular nerve cell.

Whereas in the first instance, Eq. (1.1) is derived for nerve cylinders, its domain of application has been extended to cover neurons with branching dendritic trees. Provided the diameters of the parent cylinder (d_0) and those of the daughter cylinders $(d_1, d_2, \ldots)$ at each branch point satisfy the condition

$$d_0^{3/2} = d_1^{3/2} + d_2^{3/2} + \ldots, \tag{1.2}$$

the potential over the entire dendritic tree can be obtained by solving a single cable equation of the form (1.1) if certain symmetry requirements are met. This is the transformation to the equivalent cylinder of Rall (1962). Furthermore, for a neuron with a single dendritic tree, the potential on the primary dendritic trunk may still be obtained by solving (1.1) even when many of the symmetry requirements on the input current density and the boundary conditions at the dendritic terminals are relaxed (Jack et al., 1975; Walsh and Tuckwell, 1983). As a further extension, if a neuron has several dendritic trees emanating from a common soma, the somatic depolarization can still be found by solving (1.1) (Jack et al., 1975 ; Walsh and Tuckwell, 1983). Thus when we consider (1.1) with a given input current density and given boundary conditions, the results apply in the first instance to a single nerve cylinder, but they may also apply to neurons with branching dendritic trees (see also Rinzel and Rall, 1974).

We have commenced a study of the response of a spatially extended neuron to random input currents. Thus far, we have described methods for computing the statistical properties of the depolarization $V(x,t)$ satisfying Eq. (1.1) with white noise current injection at a point x_0,

$$V_t = -V + V_{xx} + \delta(x-x_0)\left(a + b\frac{dW}{dt}\right), \quad 0<x<L, \quad (1.3)$$

where $W(t)$ is a standard (one parameter) Wiener process, and a and b are constants. Our approach (Wan and Tuckwell, 1979) was through the Fourier decomposition of $V(x,t)$

$$V(x,t) = \sum_n V_n(t)\phi_n(x), \quad (1.4)$$

where $\{\phi_n(x)\}$ is the set of spatial eigenfunctions for the cable equation with the given boundary conditions and $\{V_n(t)\}$ is the corresponding set of random Fourier coefficients. In a subsequent study (Tuckwell and Wan, 1980), we considered the effects of spatially distributed inputs (synapses) and the interaction between them. Our work so far, however, has concentrated on subthreshold depolarizations only, or depolarization in the absence of a threshold for action potential generation. In this paper we study the firing time problem for a nerve cell whose depolarization satisfies (1.3) with an assigned threshold condition. There are several methods available and we investigated the following:

(i) Solutions of the partial differential equations for the moments of first passage time for the sum of the first two terms in (1.4).

(ii) Simulation of the solution of (1.3) using N Fourier components ($N \geq 2$).

(iii) Simulation of the solution of (1.3) via a stochastic integral involving the Green's function.

2 The Moments of the Firing Time

As in our previous study (Wan and Tuckwell, 1979), we will consider a nerve cylinder whose depolarization satisfies (1.3), with initial value zero

$$V(x,0) = 0, \quad (2.1)$$

and with sealed end conditions at x = 0 and x =L,

$$V_x(0,t) = V_x(L,t) = 0. \quad (2.2)$$

Then the Fourier series for $V(x, t)$ takes the form,

$$V(x,t) = \sum_{k=0}^{\infty} V_k(t)\phi_k(x), \quad (2.3)$$

where

$$\phi_k(x) = \begin{cases} 1/\sqrt{L}, & (k=O) \\ \sqrt{2/L}\cos(k\pi x/L), & (k= 1,2, \ldots) \end{cases} \quad (2.4)$$

and the Fourier coefficients, $V_k(t), k=0, 1,2, \ldots$, are defined through the ordinary stochastic differential equations

$$dV_k = [-\mu_k^2 V_k + a\phi_k(x_0)]dt + b\phi_k(x_0)dW, \quad V_k(0) = 0. \quad (2.5)$$

The constants $\mu_k^2, k=0, 1,2, \ldots$, are the eigenvalues of the relevant boundary value problem. For reflecting ends, we have

$$\mu_k^2 = 1 + k^2\pi^2/L^2. \quad (2.6)$$

Each $V_k(t), k=0, 1, \ldots$, is an Ornstein-Uhlenbeck process.

For a fixed point of "observation", $x = \bar{x}$, we set

$$X_k(t) = V_{k-1}(t)\phi_{k-1}(\bar{x}). \quad (2.7)$$

The system of Eqs. (2.5) can be written in terms of these new variable as

$$dX_k = [-\mu_{k-1}^2 X_k + a\phi_{k-1}(\bar{x})\phi_{k-1}(x_0)]dt + b\phi_{k-1}(\bar{x})\phi_{k-1}(x_0)dW, \quad (k=1,2,\ldots). \quad (2.8)$$

2.1 *Partial Differential Equations for the Morments of the First Exit Time*

Consider a vector valued diffusion process $X(t) = (X_1(t), X_2(t), \ldots, X_n(t))$ defined by the system of stochastic ordinary differential equations

$$dX(t) = f(X(t))dt + G(X(t))dW(t), \quad (2.9)$$

where $\mathbf{f}(\cdot)$ is a deterministic n-vector, $G(\cdot) = [G_{ij}(\cdot)]$ is a deterministic $n \times n$ matrix and the components of $W(t) = (W_1(t), \ldots, W_n(t))$ are standard independent Wiener processes with covariance relations

$$E[dW_i(t)dW_j(t)] = \delta_{ij}dt, \quad (i,j=1,\ldots, n). \quad (2.10)$$

Assume that conditions for the existence and uniqueness of the solution of the system of Eq. (2.9) (see Gihman and Skorohod, 1972, for example) hold. Then if we use the Ito definition of stochastic integral (Ito, 1951) in the interpretation of the stochastic equations (2.9), the diffusion (or backward Kolmogorov) operator for the process $\mathbf{X}(t)$ is

$$\mathscr{L}_{\mathbf{z}} \equiv \sum_{i=1}^{n} f_i(\mathbf{z}) \frac{\partial}{\partial z_i} + \frac{1}{2} \sum_{i=1}^{n} \sum_{j=1}^{n} g_{ij}(\mathbf{z}) \frac{\partial^2}{\partial z_i \partial z_j}, \tag{2.11}$$

where

$$g_{ij}(\mathbf{z}) = \sum_{k=1}^{n} G_{ik}(\mathbf{z}) G_{jk}(\mathbf{z}). \tag{2.12}$$

Suppose that at t=0, X(O) $=\mathbf{z}$ where z is a point within some open set A in R^n. Let $\tau_A(\mathbf{z})$ be the first exit time of $\mathbf{X}(t)$ from A so that

$$\tau_A(\mathbf{z}) = \inf\{t | \mathbf{X}(t) \notin A,\ \mathbf{X}(0) = \mathbf{z} \notin A\} \tag{2.13}$$

We assume $\tau_A(\mathbf{z}) < \infty$ with probability one. Denoting the m^{th} moment of $\tau_A(\mathbf{z})$ by $T_m(\mathbf{z})$, *we* have the following system of equations for the moments of $\tau_A(\mathbf{z})$:

$$\mathscr{L}_{\mathbf{z}} T_m(\mathbf{z}) = -m T_{m-1}(\mathbf{z}), \qquad m = 1,2, \ldots . \tag{2.14}$$

where $T_0(\mathbf{z}) = 1$ and $\mathscr{L}_{\mathbf{z}}$ is as given by (2.11) (Gihman and Skorohod, 1972). This system is solved with the conditions that $T_m(\mathbf{z})$ is bounded and continuous in A and that $T_m(\mathbf{z})$ *0* for z on ∂A, the (finite) boundary of A. The latter condition holds because A is an open set and exit from A has already occurred if $\mathbf{z} \in \partial A$.

Upon setting $W(t) = W_1(t)$ we can put the system (2.8) in the same form as (2.9) if we set

$$f_k(\mathbf{X}) = -\mu_{k-1}^2 X_k + a\phi_{k-1}(\bar{x})\phi_{k-1}(x_0), \tag{2.15}$$

and

$$G_{i1} = b\phi_{i-1}(x_0)\phi_{i-1}(\bar{x}) \qquad (i = 1, 2, \ldots, n), \tag{2.16}$$

$$G_{ij} = 0 \qquad (i = 1, 2, \ldots, n; j = 2, 3, \ldots, n). \tag{2.17}$$

The moments of the first exit time for the n^{th} partial sum of the depolarization of the neuron at a point $\bar{x}$ can therefore be obtained from (2.1 l), (2.12), and (2.14) with $f_k(\cdot)$ and $G_{ij}(\cdot)$ given by (2.15)-(2.17).

2.2 *Time of Firing in the Two-Component Approximation*

For the purposes of describing methods of solution of the equations for the moments of the first exit time, we will restrict our attention to the case where the number of components in the system (2.8) is two. That is, we will work with the approximation to $V(\bar{x}, t)$,

$$\tilde{V}(\bar{x}, t) = X_1(t) + X_2(t). \tag{2.18}$$

We assume that the neuron fires an action potential when $\tilde{V}$ first reaches a constant threshold value θ, though there are many possible assignments of a threshold condition in cable models (Jack et al., 1975). Then, if $X_1(0) = z_1$ and $X_2(0) = z_2$, the equations for the moments, $m = 1,2, \ldots$, of the time $\tau_A(z_1, z_2)$ at which $V(\bar{x}, t)$ first reaches 8 are

$$\begin{aligned}
&[a\phi_0(\bar{x})\phi_0(x_0) - \mu_0^2 z_1] \frac{\partial T_m}{\partial z_1} \\
&\quad + [a\phi_1(\bar{x})\phi_1(x_0) - \mu_1^2 z_2] \frac{\partial T_m}{\partial z_2} \\
&\quad + \frac{b^2}{2}\left[\phi_0^2(\bar{x})\phi_0^2(x_0) \frac{\partial^2 T_m}{\partial z_1^2}\right. \\
&\quad + 2\phi_0(\bar{x})\phi_0(x_0)\phi_1(\bar{x})\phi_1(x_0) \frac{\partial^2 T_m}{\partial z_1 \partial z_2} \\
&\quad \left. + \phi_1^2(\bar{x})\phi_1^2(x_0) \frac{\partial^2 T_m}{\partial z_2^2}\right] = -m T_{m-1},
\end{aligned} \tag{2.19}$$

where $(z_1, z_2) \in A$ and $A = [(a_1, a_2) | a_1 + a_2 < \theta]$. That is, the neuron has initially a subthreshold value of $\tilde{V}(\bar{x}, t)$. In most of our applications the trigger zone' will be assumed to be at the origin $\bar{x}$ =O.

3 **Methods of Solution of the Moment Equations**

For a numerical solution of the Eq. (2.19) it is convenient to set

$$x_1 = \frac{1}{\sqrt{2}}(z_1 + z_2), \qquad x_2 = \frac{1}{\sqrt{2}}(-z_1 + z_2) \tag{3.1}$$

and write (2.19) as

$$\begin{aligned}
&\frac{b^2}{4L^2}\left(c_s^2 \frac{\partial^2 T_m}{\partial x_1^2} + 2c_s c_d \frac{\partial^2 T_m}{\partial x_1 \partial x_2} + c_d^2 \frac{\partial^2 T_m}{\partial x_2}\right) \\
&\quad - \left[\left(1 + \frac{\pi^2}{2L^2}\right) x_1 + \frac{\pi^2}{2L^2} x_2 - \frac{a c_s}{\sqrt{2} L}\right] \frac{\partial T_m}{\partial x_1} \\
&\quad - \left[\frac{\pi^2}{2L^2} x_1 + \left(1 + \frac{\pi^2}{2L^2}\right) x_2 - \frac{a c_d}{\sqrt{2} L}\right] \frac{\partial T_m}{\partial x_2} \\
&= -m T_{m-1}, \qquad (m = 1,2, \ldots)
\end{aligned} \tag{3.2}$$

with

$$\begin{aligned}
c_s &= 1 + 2\cos\left(\frac{\pi \bar{x}}{L}\right)\cos\left(\frac{\pi x_0}{L}\right), \\
c_d &= -1 + 2\cos\left(\frac{\pi \bar{x}}{L}\right)\cos\left(\frac{\pi x_0}{L}\right),
\end{aligned} \tag{3.3}$$

and $T_0(x_1, x_2) = 1$. The solution domain is now $-\infty < x_1 < \theta/\sqrt{2}$ and $-\infty < x_2 < \infty$. Along the finite

boundary (the threshold) of the domain we have

$$T_m\left(\frac{\theta}{\sqrt{2}}, x_2\right)=0, \quad (|x_2|<\infty). \tag{3.4}$$

For any point in the finite x_1, x_2-plane with $x_1<\theta/\sqrt{2}$, we have $T_m>0$ for a one-sided exit. Intuitively, T_m increases as the (transformed) initial state (x_1, x_2) moves away from the threshold $x_1=\theta/\sqrt{2}$ and T_m cannot remain bounded as $|x_1|\to$ co. However, to the extent that the process cannot exit except through the single threshold $X_1(t)+X_2(t)=\theta$, *we expect* the "limiting" boundary at infinity away from the threshold to act like a reflecting barrier so that the normal derivative of T_m tends to zero in the limit:

$$\lim_{\varrho\to\infty}\frac{\partial T_m}{\partial \varrho}=0, \quad \left(\frac{\pi}{2}<\phi<\frac{3\pi}{2}\right) \tag{3.5}$$

with $\varrho^2=(x_1-\theta/\sqrt{2})^2+x_2^2$ and $\tan\phi=x_2/(x_1-\theta/\sqrt{2})$. The PDE (3.2), the absorbing barrier condition (3.4) and the (limiting) reflecting barrier condition (3.5) determine $T_m(x_1, x_2)$.

3.1 *Perturbation Method for Small Input Variability*

When the standard deviation of the input is sufficiently small compared to the mean input so that $\varepsilon\equiv b^2/2a^2\ll 1$, the boundary value problem (BVP) for determining the mean interspike time T_1 is in the form of a singular perturbation problem and an approximate solution by the method of matched asymptotic expansions (Kevorkian and Cole, 1981) is appropriate. An *outer* (asymptotic expansion of the) *solution* for the problem may be obtained by a regular perturbation series expansion of the form

$$T_1(x_1, x_2; \varepsilon)=\sum_{n=0}^{\infty} T_1^{(n)}(x_1, x_2)\varepsilon^n, \tag{3.6}$$

where the coefficients, $T_1^{(n)}(x_1, x_2)$, $n=0, 1, 2, \ldots$, are determined by

$$P(x_1, x_2)\frac{\partial T_1^{(n)}}{\partial x_1}+Q(x_1, x_2)\frac{\partial T_1^{(n)}}{\partial x_2}=R^{(n)}(x_1, x_2) \tag{3.7}$$

with

$$P(x_1, x_2)=\left(1+\frac{\pi^2}{2L^2}\right)x_1+\frac{\pi^2}{2L^2}x_2-c_s\frac{a}{\sqrt{2}L},$$

$$Q(x_1, x_2)=\frac{\pi^2}{2L^2}x_1+\left(1+\frac{\pi^2}{2L^2}\right)x_2-c_d\frac{a}{\sqrt{2}L},$$

$$R^{(0)}(x_1, x_2)=1, \tag{3.8}$$

$$R^{(n)}(x_1, x_2)=\frac{a^2}{2L^2}\left(c_s^2\frac{\partial^2 T^{(n-1)}}{\partial x_1^2}+2c_sc_d\frac{\partial^2 T^{(n-1)}}{\partial x_1\partial x_2}+c_d^2\frac{\partial^2 T^{(n-1)}}{\partial x_2^2}\right) \quad (n\geqq 1).$$

The first order linear PDE (3.7) for $T_1^{(n)}$ may be solved by the method of characteristics. For the range of parameter values of physiological interest, $P(x, y)$ and $Q(x, y)$ do not vanish simultaneously inside the solution domain. In that case, an outer solution, satisfying all the auxiliary conditions of the original BVP except for the condition $T_1(\alpha, x_2)=0$ with

$$x_2>t_c=-\left(1+\frac{2L^2}{\pi^2}\right)\alpha+\frac{2L^2}{\pi^2}\left(\frac{ac_s}{\sqrt{2}L}\right) \tag{3.9}$$

along the threshold, can be found. An *inner* (asymptotic expansion of the) *solution* for the problem is only needed in a narrow region adjacent to $x_2>t_c$ along the threshold to satisfy the condition T_1 0 there.

For the mean interspike time, we need only the value of $T_1^{(n)}$ at the origin as we consider only a neuron which is at rest initially and returns to the resting state after firing. Therefore, we only have to compute the outer solution along the unique characteristic base curve of (3.7) which passes through the origin of the (x_1, x_2)-plane. For other purposes, more information concerning the outer solution is required. For example, the unknown values of the outer solution along three sides of the rectangle $(-\beta\leqq x_1\leqq\alpha, -\delta\leqq x_2\leqq\gamma)$ other than x_1 a are needed in the next subsection for a finite difference solution of the original BVP for $T_1(x_1, x_2)$. A detailed description of the solution scheme for computing the outer solution can be found in Wan et al. (1983). For $\varepsilon\leqq$ 0.1, a two-term approximation of the outer solution for $T_1(x_1, x_2)$ is usually adequate in application.

3.2 *Finite Difference Method for Moderate to Large Input Variability*

To compute the solution of the BVP for T_1 when ε is not necessarily small compared to unity, we have to deal with the difficulty of an unbounded solution domain. The method of Fourier transforms is not applicable here as T_1 does not vanish at $x_2=\pm\infty$. A Laplace transform in x_1 does not lead to useful simplifications. Our approach here is to seek the solution of the same PDE for T_1 only in the rectangle $(-\beta\leqq x_1\leqq\alpha, -\delta\leqq x_2\leqq\gamma)$ with $T_1=0$ along $x_1=\alpha$ as before. Along the other three *artificial* boundary lines of the rectangle, the solution is required to attain the asymptotic value of T_1 at distance far away from the origin (with $x_1<\alpha$). The determination of the asymptotic behaviour of T_1 can be found in Wan et al. (1983). We note here only the fact that, as a first approximation of the asymptotic behaviour, we may take $\partial T_1/\partial n=0$ along the three artificial boundary lines ($x_1=-\beta, x_2=-\delta$ and $x_2=\gamma$) of the rectangle.

A finite difference solution may now be sought for the new BVP on the finite rectangle in the x_1, x_2-plane.

With the first derivative terms in the PDE, a central difference scheme is known to lead to spurious oscillatory behavior and numerical instability in the (approximate) solution for $\varepsilon \ll 1$ unless the mesh is sufficiently (and uneconomically) fine. Therefore, upwind differencing is used for the first derivative terms in the finite difference scheme. The resulting system of linear equations is efficiently solved by the method of conjugate gradient with the coefficient matrix preconditioned for rapid convergence. The results obtained by the above finite difference method of solution differ by 5 % or less from a two-term perturbation solution whenever $\varepsilon \leqq 0.1$. Similar agreements with results from the simulation method, to be described in the next section, have also been verified.

4 **Simulation Methods of Solution**

4.1 *Simulation Via the Fourier Series*

The methods of solution described in Sect. 3 for asymptotic and finite difference solutions of the expected first passage time of the n^{th} partial sum approximation for the nerve cell depolarization evidently become either very tedious and costly or intractable for $n > 3$. Furthermore, the determination of the second moment of the first passage time involves still more analysis and machine computation beyond the solution for the first moment. It is therefore useful to consider approximate solutions of the same first passage time problem by computer simulations.

For the purpose of computer simulations, the stochastic differential equation for the individual component O.U.P. $X_k(t)$,

$$dX_k(t) = [-\mu_{k-1}^2 X_k(t) + a\phi_{k-1}(\bar{x})\phi_{k-1}(x_0)]dt + b\phi_{k-1}(\bar{x})\phi_{k-1}(x_0)dW \tag{4.1}$$

is approximated by

$$X_k(t+\Delta t) - X_k(t) = [-\mu_k^2 X_k(t) + a\phi_{k-1}(\bar{x})\phi_{k-1}(x_0)]\Delta t + b\phi_{k-1}(\bar{x})\phi_{k-1}(x_0)[W(t+\Delta t) - W(t)] \tag{4.2}$$

In the limit as $\Delta t \to 0$, the stochastic difference Eq. (4.2) gives the correct interpretation of the stochastic differential equation in relation to the (Ito) stochastic integral. We start with the initial condition $X_k(0)$ 0 and generate $X_k(m\Delta t)$ by

$$X_k(m\Delta t) = X_k((m-1)\Delta t) + [-\mu_{k-1}^2 X_k((m-1)\Delta t) + a\phi_{k-1}(\bar{x})\phi_{k-1}(x_0)]\Delta t + b\phi_{k-1}(\bar{x})\phi_{k-1}(x_0)N_m\sqrt{\Delta t}, \quad (m = 1,2,\ldots). \tag{4.3}$$

where $N_m, m = 1, 2, \ldots,$ are independent standard norma1 random variables. Realizations of these random variables are generated by random number generator routines.

The n^{th} partial sum of the nerve cell depolarization at a point $\bar{x}, U_n(\bar{x}, t)$, is given by

$$U_n(\bar{x}, t) = \sum_{k=0}^{n-1} V_k(t)\phi_k(\bar{x}) = \sum_{k=1}^{n} X_k(t). \tag{4.4}$$

The difference Eqs. (4.3) with $k = 1,2, \ldots, n$, for the component Ornstein-Uhlenbeck processes $X_k(t)$ enable us to obtain histograms of first passage times for $U_n(\bar{x}, t)$ and to estimate the corresponding first exit time moments. The results for U_2 provide a useful check for results obtained by the methods described in Sect. 3. In addition, the effects of adding more terms in the series representation for $V(\bar{x}, t)$ may be examined. The choice of Δt is arbitrary but in practice smaller and smaller values are tried until consistency requirements are met.

4.2 *Simulation Via the Green's Function Representation*

An alternative to simulating the solution of (1.3) by its Fourier components is to' appeal directly to the Green's function representation of the solution. Letting $G(x, \xi; t - s)$ denote the Green's function for (1.1) and the given boundary conditions and assuming the depolarization is initially zero, we have,

$$V(x, t) = \int_0^t G(x, x_0, t-s)\left[a + b\frac{dW(s)}{ds}\right]ds. \tag{4.5}$$

The depolarization is thus the sum of a deterministic component, $V_D(x,t)$, and a random component, $V_R(x,t)$,

$$V(x,t) = V_D(x,t) + V_R(x,t), \tag{4.6}$$

where

$$V_D(x,t) = a\int_0^t G(x, x_0; t-s)ds \tag{4.7}$$

and

$$V_R(x,t) = b\int_0^t G(x, x_0; t-s)dW(s). \tag{4.8}$$

Here (4.7) involves the usual Riemann integral whereas (4.8) involves the stochastic integral with respect to Wiener measure. The solution of (1.3) may thus be found directly from (4.7) and (4.8).

It is important and useful to note that there are two representations of the Green's function for (1.3). The first one, obtained by the method of images, is

$$G(x, \xi; t) = \frac{e^{-t}}{\sqrt{4\pi t}}\sum_{n=-\infty}^{\infty}\left[\exp\left\{\frac{-(x-2nL-\xi)^2}{4t}\right\} + \exp\left\{\frac{-(x-2nL+\xi)^2}{4t}\right\}\right], \tag{4.9}$$

which converges rapidly for small t. The second representation, obtained by the method of separation of variables, is

$$G(x,\xi;t)=\frac{e^{-t}}{L}\left[1+2\sum_{n=1}^{\infty}\cos\left(\frac{n\pi x}{L}\right)\cos\left(\frac{n\pi x_0}{L}\right)\right.$$
$$\left.\exp\{-n^2\pi^2t/L^2\}\right] \tag{4.10}$$

which converges rapidly for large t.

(a) The Deterministic Component. The deterministic component V_D can be obtained explicitly using either of the two representations of $G(x,\xi;t)$. For calculations at small times we have

$$V_D(x,t)=\frac{a}{2\sqrt{\pi}}\int_0^t\frac{e^{-T}}{\sqrt{T}}\sum_{n=-\infty}^{\infty}\left[\exp\left\{\frac{-\alpha_n^2}{4T}\right\}\right.$$
$$\left.+\exp\left\{\frac{-\beta_n^2}{4T}\right\}\right]dT, \tag{4.11}$$

where

$$\alpha_n=x-2nL-x_0, \tag{4.12}$$

$$\beta_n=x-2nL+x_0. \tag{4.13}$$

Using the relation,

$$\int_0^t\frac{\exp[-T-x^2/4T]}{\sqrt{T}}dT=\left[e^{-|x|}\operatorname{erfc}\left(\frac{|x|-2t}{2\sqrt{t}}\right)\right.$$
$$\left.-e^{|x|}\operatorname{erfc}\left(\frac{|x|+2t}{2\sqrt{t}}\right)\right], \tag{4.14}$$

where erfc(·) is the complementary error function,

$$\operatorname{erfc}(x)=\frac{2}{\sqrt{\pi}}\int_x^{\infty}e^{-z^2}dz, \tag{4.15}$$

which is available as a library function or subroutine in most computing centers, we obtain

$$V_D(x,t)=\frac{a}{4}\sum_{n=-\infty}^{\infty}\left[e^{-|\alpha_n|}\operatorname{erfc}\left(\frac{|\alpha_n|-2t}{2\sqrt{t}}\right)\right.$$
$$-e^{|\alpha_n|}\operatorname{erfc}\left(\frac{|\alpha_n|+2t}{2\sqrt{t}}\right)$$
$$+e^{-|\beta_n|}\operatorname{erfc}\left(\frac{|\beta_n|-2t}{2\sqrt{t}}\right)$$
$$\left.-e^{|\beta_n|}\operatorname{erfc}\left(\frac{|\beta_n|+2t}{2\sqrt{t}}\right)\right]. \tag{4.16}$$

For large times a formula suitable for calculating of V_D is obtained from (4.10) :

$$V_D(x,t)=\frac{a}{L}\left[1-e^{-t}+2\sum_{n=1}^{\infty}\frac{\cos(n\pi x/L)\cos(n\pi x_0/L)}{1+n^2\pi^2/L^2}\right.$$
$$\left.\cdot\{1-\exp(-(1+n^2\pi^2/L^2)t)\}\right]. \tag{4.17}$$

Accelerated convergence can be achieved by writing this as the sum of steady state and transient solutions:

$$V_D(x,t)=V_{DS}(x,x_0)$$
$$-e^{-t}\left[1+2\sum_{n=1}^{\infty}\frac{\cos(n\pi x/L)\cos(n\pi x_0/L)}{1-n^2\pi^2/L^2}\right.$$
$$\left.\exp\{-n^2\pi^2t/L^2\}\right], \tag{4.17A}$$

where

$$V_{DS}(x,x_0)=\begin{cases}\dfrac{a\cosh(L-x_0)\cosh(x)}{\sinh(L)} & (x<x_0)\\[2ex] \dfrac{a\cosh(x_0)\cosh(L-x)}{\sinh(L)} & (x>x_0).\end{cases} \tag{4.17B}$$

(b) The Random Component. The definition of stochastic integral gives

$$V_R(x,t)=b\int_0^t G(x,x_0;t-s)dW(s)$$
$$=\lim_{n\to\infty}\sum_{k=0}^{n-1}bG(x,x_0;t-k\Delta s)$$
$$\cdot[W((k+1)\Delta s)-W(k\Delta s)], \tag{4.18}$$

where the limit is in mean square and where $\Delta s=t/n$. Thus the random component may be approximated by the random sum

$$\tilde{V}(x,t)=b\sum_{k=0}^{n-1}G(x,x_0;(n-k)\Delta s)$$
$$[W((k+1)\Delta s)-W(k\Delta s)]$$
$$=b\sqrt{\Delta s}\sum_{k=0}^{n-1}G(x,x_0;(n-k)\Delta s)N_k, \tag{4.19}$$

where $N_0,N_1,\ldots$ is a set of independent standard normal random variables.

We may now simulate the solution of (1.3) directly. The deterministic component V_D, which is the expected value of V, can be obtained to desired accuracy. For small values of t formula (4.16) is employed and for large values of t formula (4.17) is employed. The same procedure is employed for the simulation of V_R in that one switches representations of the Green's functions for some intermediate value of t, thus obtaining an extremely rapid convergence for all t and avoiding the difficulty of the slow convergence of the Fourier series for small t.

5 Results

5.1 Comparison of the Mean Firing Times Obtained by the Three Methods

We shall consider a nerve cylinder of total electrotonic length $L=2$ with an input current of mean $a=10$

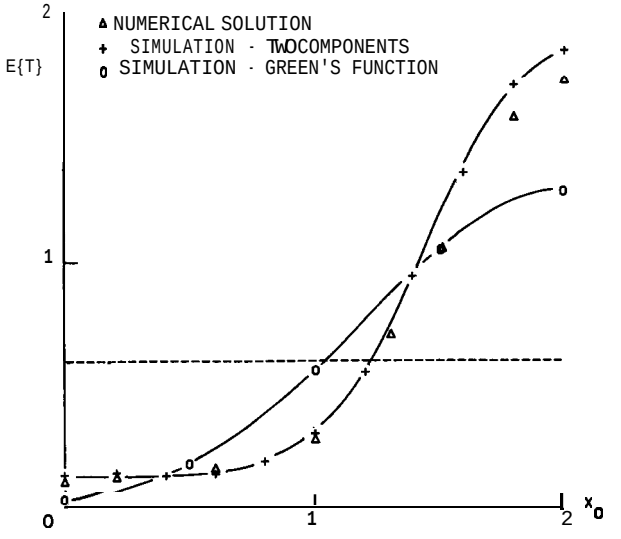

Fig. 1. Mean interspike interval for various input positions x_0 calculated by three different methods. (△) Numerical solution of the partial differential equation for the mean with two terms in the Fourier series. (+) Simulation results for two terms in the Fourier series. (○) Simulation results using the Green's function representation of the solution. Parameter values: $a=10$, $b=1$, $L=2$, $\theta=\sqrt{2}$. The horizontal dashed line is the result for just the first term in the Fourier series

and standard deviation $b = 1$. For this parameter set, we compare the mean interspike interval obtained by the three methods of solutions:

(i) The finite difference solution of the partial differential Eq. (2.19) for the mean with two components of the Fourier series.

(ii) Simulation of the first two components of the Fourier series.

(iii) Simulation of the solution of (1.3) by using the Green's function representation (4.5) for the solution.

The firing time, or interspike interval, which we shall henceforth designate by T, is taken as the time for the depolarization at the origin to reach the threshold value $\theta=\sqrt{2}$. (The use of this threshold value is for numeri.cal convenience and it should be noted that θ can be scaled by an arbitrary numerical factor so long as a and b are similarly scaled whereupon the value of T will be the same.) At the same time we will investigate the dependence of the expected firing time on input position, though, with our value of $b/a = 0.1$ this dependence will be primarily deterministic (low input variability).

The results obtained by the three methods, (i)-(iii), for various values of the position x_0, of the white noise input, are shown in Fig. 1. The horizontal dashed line, giving $E[T] \cong 0.597$, corresponds to the result for a one term Fourier series solution.

The results for the two-component simulation (marked by +) were obtained with sample sizes of $N = 500$ and with Δt [in (4.3)] = 0.0005 for $0 \leqq x_0 \leqq 1$ but Δt =O.OOl for $1 < x_0 \leqq 2$. (We have found that the larger time step $\Delta t = 0.001$ is adequate for $1 < x_0 \leqq 2$ as E[T] is larger for that range.) With $x_0 = 0$, the mean firing time is E[T] = 0.108 + 0.003 (95 % confidence intervals) and with $x_0 = 2$ we-have E[T] = 1.83 +0.02.

For the simulations via the Green's function (which we will refer to as the "full solution") the sample sizes for the mean firing time were N= 200 with Δs [in (4.19)]=0.001 for $0 \leqq x_0 \leqq 1$ and $\Delta s = 0.01$ for $1 < x_0 \leqq 2$. With x_0 0 the mean firing time was E[T] = 0.0094 ± 0.0012 and with $x_0 = 2$ we have E[T]=1.29 ±0.02.

Inspection of Fig. 1 shows that there is excellent agreement between the values of E[T] for the two-component approximation obtained by solving the partial differential Eq. (2.19) and those by simulation of the corresponding system of ordinary stochastic differential equations. The agreement is best for small values of x_0; for the worst case, $x_0 = 2$, the difference is only 6%. Thus these two sets of results mutually support their accuracy in the determination of the mean firing time in the two-component approximation.

When we compare the results for the two-component approximation with those obtained by simulating the full solution of the stochastic partial differential Eq. (1.3) we see that :

(a) for small values of x_0 (less than 0.3) the results for the two-component approximation are larger than those for the full solution. For example, when $x_0 = 0$, the mean firing time for the full solution is only 8.7 % of that for the two-component approximation ;

(b) for intermediate values of x_0 ($0.3 \leqq x_0 \leqq 1.5$), values of E[T] for the two-component approximation are somewhat less than those for the full simulated solution ;

(c) for large values of x_0 ($x_0 > 1.5$), values of E[T] for the two-component approximation are somewhat greater than those for the full simulated solution.

(d) near x_0 =0.5 and x_0 = 1.5, the two-component results are very accurate (see also discussion in Sect. 5.2).

The fact that (a) occurs is readily explainable because small values of x_0 correspond to small first passage times and it is known that the sum of the first two Fourier components will be an inadequate approximation to the full solution for small t. This point will be elaborated upon below.

To explain (b) and (c) it is only necessary to examine, for the chosen parameter values, the stochastic differential equation for the second component of the Fourier series. From (2.8) this is, with x 0 and

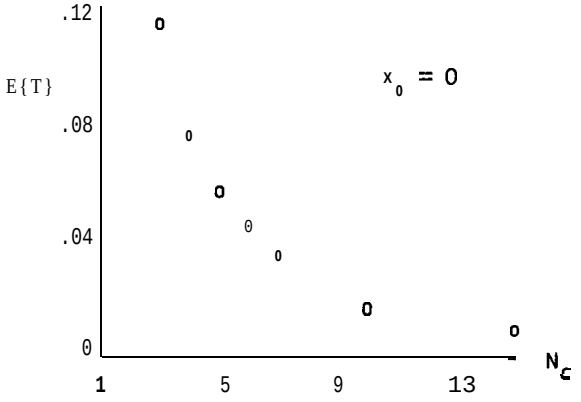

Fig. 2. Mean interspike interval from simulation of Fourier series as the number of terms is increased. In this case the input is at $x_0 = 0.0$, the interspike interval is small and the convergence to the mean obtained with the full simulated solution is slow. Parameter values: a = 20, b = 10, L = 1, $\theta = 10$

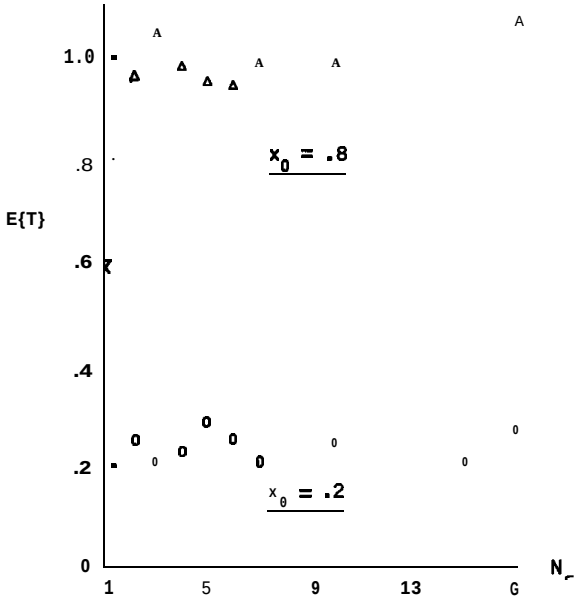

Fig. 3. Mean interspike interval from simulation of Fourier series as the number of terms is increased. The point marked x is the result for just one term and is independent of input position. The upper set of results (A) is for an input at $x_0 = 0.8$, the lower set (0) for $x_0 = 0.2$, the remaining parameters being as in Fig. 2. In these cases the interspike interval is large, so that the first few terms in the Fourier series are sufficient to give an accurate estimate of the mean interspike time obtained from the full simulated solution (G)

L=2,

$$dX_2 = \left[-\left(1 + \frac{\pi^2}{4}\right) X_2 + a\cos(\pi x_0/2) \right] dt + b\cos(\pi x_0/2) dW. \quad (5.1)$$

When a= 10 and b= 1 the predominant effect will be that of the drift $a\cos(\pi x_0/2)$. When $x_0 < 1$ this drift is positive which will, in anticipation of further terms in the Fourier series, tend to make the first passage time smaller. On the other hand, when $x_0 > 1$, this drift is negative, which tends to make the first passage time larger. The fact that $x_0 = 1$ is not the precise location of the cross over of the two-component results and those of the full solution is due to contributions from the noise term.

Independent of the method of solution, the mean firing time increases by at least an order of magnitude as the input position increases from $x_0 = 0$ to $x_0 = L$. This was confirmed by calculations for L = 0.5, 1.0, and 1.5, which are not reproduced here.

5.2 *Dependence of the Interspike Interval on the Number of Terms in the Fourier Series*

In order to examine the dependence of the interspike interval on the number of terms included in the Fourier series for $V(0, t)$, we performed simulations with various numbers of terms in (4.4). The parameter values were set at $L = 1$, $a = 20$, $b = 10$ with a threshold voltage $\theta = 10$ mV at the origin. Simulations were performed with various input positions, x_0.

In Fig. 2 we show the mean interspike intervals for $x_0 = 0$, retaining N_c number of terms in the Fourier series with $N_c \leqq 15$. In this case the calculated mean firing time decreases rapidly as the number of terms in the series increases. The mean firing times for $N_c = 1$ and $N_c = 2$ are beyond the range of the figure. Although the value of $E[T]$ has dropped to 0.00961 when N_c = 15, this value is still much higher than the value $E[T] = 0.0027$ obtained with the full simulated solution. The explanation for the slow convergence of $E[T]$ as N_c increases is that, in this case, the time to reach threshold is small and the Fourier series converges slowly for small values of t. The same remarks made for the mean are applicable to the standard deviation of the firing time and also its histogram.

The corresponding sets of results for input positions x_0 =0.2 and x_0 =0.8 are shown in Fig. 3. The point marked G on the N_c scale corresponds to the case when the solution is simulated via the Green's function. For these more remote input positions, the mean interspike time shows an oscillatory behavior as N_c increases. It can be seen that the mean interspike times obtained when only two terms are included in the Fourier series are in reasonable agreement with the results obtained for the full simulated solution (G).

Notice that when $N_c = 1$, in which case the depolarization is a single Ornstein-Uhlenbeck process, the interspike time is independent of input position and its expectation in this case is E[T]=0.597. This point is marked X in Fig. 3. The inclusion of one more term in the Fourier series is sufficient to take this to a

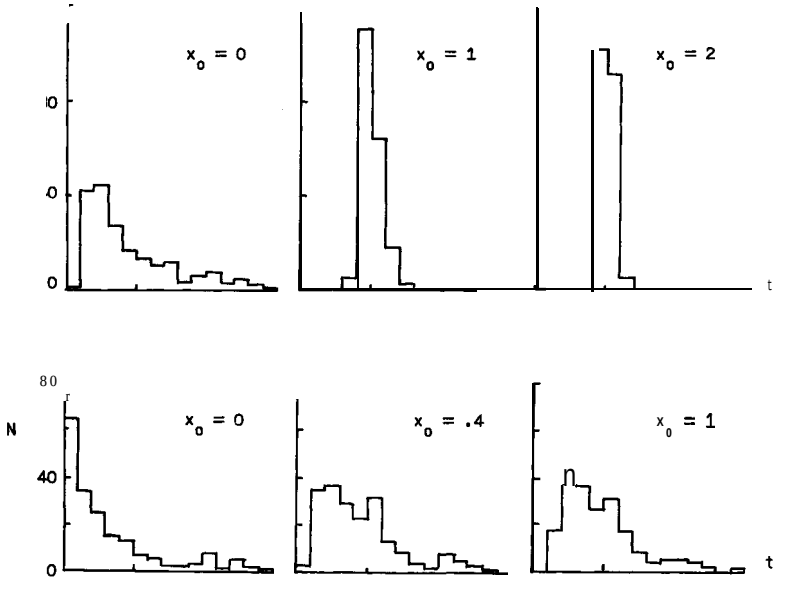

Fig. 4. Interspike interval histograms obtained by simulation of the depolarization for various input positions. In each case the bin width is one fifth of the mean interval and the mean is indicated on the horizontal axis. In the upper set of results the parameter values are a= 10, b=1, L= 2, $\theta = \sqrt{2}$. For the three lower histograms the parameter values are: $a = 20$, $b = 10$, $L = 1$, and $\theta = 10$

value close to that obtained with the full solution when x_0 =0.2 or x_0 =0.8 (but not when $x_0 = 1$, because X_2 0 in this case).

A word of caution concerning the simulations with regard to their dependence on Δt is appropriate, especially when the number of Fourier components is large. To illustrate, consider the following set of results when $x_0 =$ 0.8 with 15 components in the Fourier series and with remaining parameter values as cited at the beginning of this subsection. For Δt values of 0.005, 0.0025, and 0.001, the values of E[T} were 0.0233, 0.295, and 0.979, respectively. Only the last of these values is plausible (see Fig. 3). The anomalous results for the larger values of Δt are due to a randomly occurring early large ΔW. When this occurs in each of the 15 components, $V(0,t)$ is taken to threshold in just a few time steps. It is possible that the value E[T] = 0.979 obtained with $\Delta t =$ 0.001 is also somewhat low due to this phenomenon (approximation of a continuous time process by a discrete time one).

The general principle emerges that one term alone in the Fourier series will rarely be sufficient for a reasonably accurate value of E[T] (or T); that two terms will yield a good approximation whenever the interspike time is fairly large; and that if the interspike time is very small then the full solution should be used or possibly that obtained by using the Green's function representation (4.9). In other words, the principles governing the convergence of the Green's functions, (4.9) and (4.10), also apply to the convergence of the random series.

The set of results (for $x_0 = 0$, for example) where the first few terms of the Fourier series are inadequate, however, are unlikely to coincide with real physiological situations, since such small mean interspike intervals are rarely encountered. The smallest interspike interval known to the authors is that of the Renshaw cell. This cell can fire up to 1200 impulses per second, which corresponds to an interspike interval T= 0.14 if a time constant of 6ms is assumed.

5.3 *Dependence of the Interspike Interval Density on Input Position*

The full simulated solution of (1.3) was used to investigate the dependence of the shape of the histogram of interspike intervals on input position. Some of the results obtained are shown in Fig. 4.

In the upper part of the figure the parameter values employed were $a = 10, b=1, L=2, \theta = \sqrt{2}$ and the input positions were $x_0 =$ 0.0, 1.0, and 2.0. The number of occurrences N is plotted against interspike times in such a way that the bin width is one fifth of the mean interval. The mean interval is indicated on the t-axis. This first set of parameters corresponds to small input variability.

When the white noise input is at the origin (soma or trigger zone in our work), the interspike intervals are small but there is a lot of scatter about the mean (see below). The underlying density resembles a gamma density of low order. When the input is at the midpoint of the cylinder representing the neuron, the

underlying density is skewed slightly towards smaller values and there is a noticeable absence of interspike times much smaller than and much greater than the mean. In the final case, $x_0 = 2.0$, the input is at the most remote possible location and the underlying density is Gaussian like with very little scatter, the absence of very small and very large interspike times being even more pronounced.

In the lower part of Fig. 4 are the results for the parameter values a –20, b=10, L=1, $\theta = 10$ and the input positions were $x_0 =$ 0.0, 0.4, and 1.0. When $x_0 = 0.0$, the interspike intervals are mainly concentrated at values smaller than the mean and the underlying density is exponential in character. When $x_0 = 0.4$, the histogram has become more symmetric about the mean and the very small interspike times have almost disappeared. The same remarks apply for the case $x_0 =$ 1.0 and in both of these last two cases the underlying density is gamma-like of low order.

The two most noticeable features of the histograms shown in Fig. 4 are :

(i) the shape of the interspike interval histogram (or its underlying density) shows a pronounced dependence on input position;

(ii) the histogram obtained by simulating the solution of Eq. (1.3) show a striking resemblance to many of those found for real neurons [see for example references to experimental work in Tuckwell and Richter (1978) and Cope and Tuckwell (1980)].

It is therefore possible that examination of experimental interspike interval histograms can reveal clues as to the location of active inputs and in particular their electrotonic distance from the trigger zone (soma). In studies on cochlear nucleus cells (Pfeiffer and Kiang, 1965) and cortical cells (Whitsel et al., 1972) histogram shapes were found to vary systematically with anatomical location and it is likely that one contributing factor was the corresponding change in location of active inputs on the somadendritic surfaces.

5.4 *The coefficient of Variation of the Interspike Interval*

The coefficient of variation (CV) of the interspike interval is often employed to quantify the regularity of a spike train (see for example, Goldberg et al., 1982), a completely regular train of impulses having a CV of zero. To study the dependence of the CV on input position we used the full simulated solution with parameter values as in the previous subsection.

For the parameter values a= 10, b= 1, 8 $= \sqrt{2}$, L =2, the results obtained for the mean, standard deviation (SD) and coefficient of variation for various x_0 are given in Table 1. For the second set of parameter values, a = 20, b = 10, 8 = 10, L= 1, the results are given in Table 2.

Table **1.** Mean, standard deviation, and coefficient of variation of the firing time from simulations of the full solution (200 observations). Parameter values $a =$ 10, h = 1, 8 = $\sqrt{2}$, L = 2. The input location is x_0

x_0	Mean	SD	c v
0.0	0.0094	0.0084	0.89
0.5	0.209	0.050	0.24
1.0	0.574	0.076	0.13
1.5	1.049	0.104	0.10
2.0	1.287	0.118	0.092

Table 2. Mean, standard deviation, and coefficient of variation of the firing time from simulations of the full solution (200 observations). Parameter values $a =$ 20,b = 10, θ = 10, L = 1

x_0	Mean	SD	c v
0.0	0.0027	0,0048	1.8
0.2	0.279	0.282	1.0+
0.4	0.595	0.447	0.75
0.6	0.893	0.613	0.69
0.8	1.064	0.716	0.67
1.0	1.107	0.718	0.65

Examination of these two sets of results shows that both the mean and the standard deviation of the interspike interval increase as the distance of the input from the origin increases. In contrast, the coefficient of variation decreases monotonically as the input current becomes more remote- from the trigger zone ; the output process is less noisy the further the input is from the trigger zone. This effect counters our intuition as we had expected more reliable information transmission when the input was close to, rather than remote from, the trigger zone. The somewhat surprising dependence of CV on x_0 arises because the rate of increase of the mean is greater than that of the standard deviation. Though the firing rate decreases, there is a greater tendency for the noise to be filtered out and the information transmission becomes more reliable. This is forcefully depicted in the histograms in the upper part of Fig. 4.

One other noteworthy feature of the results for the CV is that this quantity is sometimes greater than unity. It was previously conjectured on the basis of results for point models that a CV greater than unity was possible when there was excessive inhibition (Tuckwell, 1979; Wan and Tuckwell, 1982; see also Wilbur and Rinzel, 1983). The present results indicate that in spatial models a CV greater than unity can also occur in the case of a white noise input current. The cases in Table 2 where the CV is greater than unity correspond to very high firing rates.

5.5 Diffusion Approximation to Poisson Input

White noise current has been used to excite nerve cells (Bryant and Segundo, 1976) with the main purpose of analysing the current waveforms preceding spikes. In their natural state, however, most CNS neurons receive inputs at discrete times when impulses occur in presynaptic fibers. The train of inputs can, under certain circumstances, be approximated by a Poisson process. Indeed, in one experiment (Redman and Lampard, 1968), Poisson excitation of cat spinal motoneurons was achieved and the input/output frequency relation obtained.

With Poisson input at x_0 in the present model, the depolarization will satisfy the equation

$$V_t = -V + V_{xx} + \delta(x - x_0)\varepsilon \frac{d\pi_\lambda}{dt}, \tag{5.2}$$

where $\pi_\lambda(t)$ is a Poisson process with rate parameter λ and ε is a constant. Since a smoothed version of $\varepsilon d\pi_\lambda$ is $\varepsilon\lambda dt + \varepsilon\sqrt{\lambda}dW$, *we see* that a diffusion approximation (see Walsh, 1981) to (5.2) is

$$V_t = -V + V_{xx} + \delta(x - x_0)\left(\varepsilon\lambda + \varepsilon\sqrt{\lambda}\frac{dW}{dt}\right), \tag{5.3}$$

which has the same form as (1.3) with $a = \varepsilon\lambda$ and $b = \varepsilon\sqrt{\lambda}$.

We simulated solutions of (5.3) and obtained interspike intervals with $\varepsilon = 3$ and $\lambda = 2.0$, 2.5, 3.0, and 3.5. These values of λ are in the range of input frequencies employed by Redman and Lampard (1968) and the value of ε was chosen in order to give firing rates in the physiological range. (Note that if a time constant of 5 ms is assumed, then $\lambda = 1$ corresponds to a frequency of $200\,\mathrm{s}^{-1}$.) In these simulations, two input locations were employed, $x_0 = 0.3$ and $x_0 = 0.5$, as these are the approximate electrotonic distances of Ia synapses from the soma in cat spinal motoneurons (Jack et al., 1971). The results are shown in Table 3.

The mean interspike intervals were converted to output frequencies (f_{out}) by adding a refractory period of 0.2 time constants and assuming a time constant of 5 ms. These frequencies are plotted against input frequency (f_{in}) in Fig. 5 where 95 % confidence intervals are indicated.

For both input locations the firing rate is very small ($\leqq 1\,\mathrm{s}^{-1}$) for input frequencies less than $400\,\mathrm{s}^{-1}$ ($\lambda = 2$). The output frequency increases rapidly as the input frequency increases beyond $400\,\mathrm{s}^{-1}$. The rate of increases is about doubled when the input is shifted from $x_0 = 0.5$ to $x_0 = 0.3$. In both cases the output/input frequency relation is approximately linear and, as can be seen from Table 3, the CV of the interspike time decreases as f_{in} increases.

Table 3. Mean, standard deviation, and coefficient of variation of the interspike time from simulations of the full solution. Parameter values are $a = \lambda\varepsilon$, $b = \varepsilon\sqrt{\lambda}$, $\varepsilon = 3$, $\theta = 10$, $L = 1.5$

x_0		Mean	SD	c v
0.3	2.0	172.00	156.000	0.91
0.3	2.5	5.43	4.520	0.83
0.3	3.0	1.87	1.410	0.76
0.3	3.5	1.31	0.890	0.68
0.5	2.5	10.71	8.280	0.77
0.5	3.0	5.00	3.680	0.74
0.5	3.5	2.89	1.820	0.63

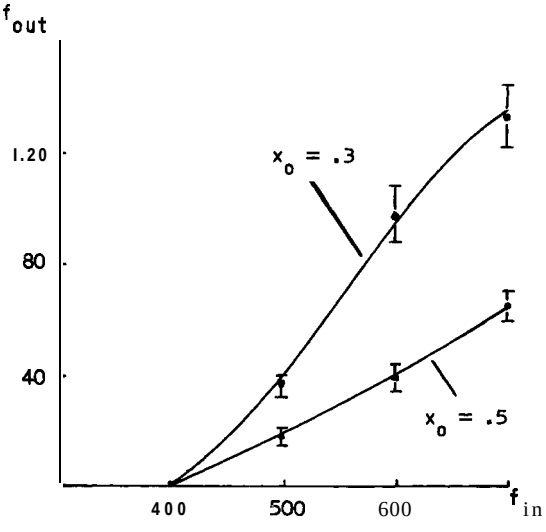

Fig. 5. Mean firing rate versus input frequency for two different input positions, $x_0 = 0.3$ and $x_0 = 0.5$. These results are for a diffusion approximation to Poisson input as described in the text. Parameter values : $L = 1.5$, $\theta = 10$; a and b depend on input frequency. A time constant of 5 ms has been assumed and a refractory period of 1 ms

We have previously mentioned (in Sect. 5.4) that the CV of the interspike interval decreases as the input becomes more remote from the soma, but at the expense of a decrease in firing rate. From the results in Table 3 we see that the mean output frequency is *greater* and the CV is less in the case of an input at $x_0 = 0.5$ with $\lambda = 3$, than when the input is at $x_0 = 0.3$ and $\lambda = 2.5$. Thus, in this case, if the input strength (frequency) at a more distal location is increased sufficiently to achieve a firing rate equal to that with a weaker input at a more proximal location, the output process is less noisy. If this result generalizes, it may indicate that more reliable output can be achieved by the placement of stronger (more) inputs at remote locations, which is a surprising result. However, we have not considered a sufficient number of examples to make this more than a conjecture which can be tested in subsequent investigations.

5.6 *Multiple Trigger Zones and Multiple Inputs*

We have also studied the effects of introducing a second trigger zone, using the full simulated solution to find the interspike interval. If the trigger zones are located at x_1 and x_2 then the firing time is taken as the minimum of the first passage times of $V(x_1, t)$ and $V(x_2, t)$ to a threshold level θ. In one such investigation we set $a = 20, b = 10$, $\theta = 10$, $L = 1$ with the input at $x_0 = 0.75$. With a single trigger zone at x_1 =O.O the interspike interval had mean, standard deviation and CV, equal to 1.02, 0.567, and 0.56, respectively (sample size 500). When a second trigger zone was introduced at $x_2 = 0.5$, all other parameter values being the same, the mean, standard deviation and CV were 0.657, 0.447, and 0.68, respectively. Thus the firing rate is increased at the expense of an increased CV. In both cases the histogram of interspike intervals was gamma like of low order and apparently unimodal.

We also considered situations where there were two input locations and two trigger zones. In such cases the firing rate was greatly enhanced but again the CV was very large. The histograms of interspike intervals turned out to be unimodal in the few cases considered.

6 **Summary and Conclusions**

We have investigated the time between action potentials for a model neuron consisting of a finite cylinder whose depolarization is governed by the linear cable equation with white noise current injection at a point. We have chosen sealed end boundary conditions at both ends of the cylinder although other types of end conditions can also be treated by the same methods used in this paper. There are many possible choices of threshold; we chose the simple one that the cell fires an action potential when the depolarization at the soma reaches threshold.

The solution of the stochastic cable equation can be written down in terms of the Green's function for any input current density. With a white noise current at a point of the form $a + bdW/dt$, where a and b are constants and W(t) is a standard Weiner process, the solution of the stochastic cable equation splits into a deterministic part, which is the mean depolarization, and a random part involving a stochastic integral with respect to W. There are two common series representations for the Green's function: one, obtained by the method of images, converges rapidly for small values of t (time) and the other, obtained by separation of variables is a Fourier series which converges rapidly for large t.

For the Fourier series solution, we use two methods of solutions to obtain the moments of the interspike time between action potentials. The first is to solve the partial differential equations for the moments (and density) of the first passage time associated with a finite number of terms in the Fourier series. When the input variability is small we have solved the moment equations by matched asymptotic expansions (though only the outer solution is needed herein). For more noisy inputs, we have obtained numerical solutions of the moment equations by finite differencing. The other method of estimating the moments of the firing time is to simulate the Fourier components by discretizing time and employing random number generators to obtain sample paths for the depolarization. We found that solutions obtained by these two different methods were in excellent agreement.

As the same principles governing the convergence of ordinary Fourier series also apply to the random Fourier series, accurate estimates of the first passage time of the somatic depolarization to threshold can be obtained with a few terms of the Fourier series providing most of the density of the first passage time is concentrated at large times. Solving the partial differential equations for the moments is recommended if only the mean interspike time is required. The determination of higher order moments is hindered by the fact that calculation of the second moment requires an accurate determination of the first, etc. The simulation of the Fourier series has the advantage of yielding estimates of the moments and the density of the interspike interval.

If there are significant contributions to the interspike interval density at small times, a more rapid convergence is obtained by simulating the solution of the stochastic partial differential equation directly using the Green's function for $t \lesssim 0.2$ but switching from the images representation to the eigenfunction expansion representation at larger times, thus obtaining rapid convergence for all t.

Using the cable model neuron has enabled us to study the effects of input position on the firing time. The strong dependence of the mean firing time on input location is predictable from deterministic studies. In addition we have found a strong dependence of the shape of the interspike interval density on input position. The histograms obtained from the simulation studies bore striking resemblance to those of real neurons, suggesting that interspike interval histogram shape may reveal clues as to the location of synaptic input. We also found a strong dependence of the coefficient of variation of the interspike interval on input position. As the distance of the input from the trigger zone increases the coefficient of variation decreases monotonically. In fact, some of our results (see Sect. *5.5)* indicate that it is possible to obtain an output interval with the same or smaller mean but a smaller

coefficient of variation from a higher input frequency at a more remote site. On this basis we conjectured that m.ore reliable information transmission, in the sense of a more regular output spike train, might sometimes be possible with inputs at distal rather than proximal locations on the dendritic tree.

Acknowledgement. The research is supported in part by Canadian NSERC Individual Operating Grant No. A9259.

References

Bryant, H.L., Segundo, J.P. : Spike initiation by transmembrane current : a white noise analysis. J. Physiol. 260, 279-314 (1976)

Capocelli, R.M., Ricciardi, L.M. : Diffusion approximation and first passage time problem for a model neuron. Kybernetik 8, 214-223 (1971)

Cope, D.K., Tuckwell, H.C. : Firing rates of neurons with random excitation and inhibition. J. Theor. Biol. 80, 1-14 (1979)

Gihman, I.I., Skorohod, A.V. : Stochastic differential equations. Berlin, Heidelberg, New York : Springer 1972

Gluss, B. : A model for neuron firing with exponential decay of potential resulting in diffusion equations for probability density. Bull. Math. Biophys. 29, 223-243 (1967)

Goldberg, J.M., Fernandez, C., Smith, C.E. : Responses of vestibular nerve afferents in the squirrel monkey to externally applied galvanic currents. Brain Res. 252, 156-160 (1982)

Hanson, F.B., Tuckwell, H.C. : Diffusion approximations for neuronal activity including synaptic reversal potentials. J. Theor. Neurobiol. 2 (1983) (in press)

Hodgkin, A.L., Rushton, W.A.H.: The electrical constants of a crustacean nerve fibre. Proc. R. Soc. B 133, 444-479 (1946)

Ito, K. : On stochastic differential equations. Mem. Am. Math. Soc. 4 (1951)

Jack, J.J.B., Miller, S., Porter, R., Redman, S.J. : The time course of minimal excitatory post-synaptic potentials evoked in spinal motoneurones by group Ia afferent fibres. J. Physiol. 215, 353-380 (1971)

Jack, J.J.B., Noble, D., Tsien, R. W. : Electrical current flow in excitable cells. Oxford: Clarendon Press 1975

Kevorkian, J., Cole, J.D.: Perturbation methods in applied mathematics. Berlin, Heidelberg, New York: Springer 1981

Pfeiffer, R.R., Kiang, N.Y.-S. : Spike discharge patterns of spontaneous and continuously stimulated activity in the cochlear nucleus of anesthetized cats. Biophys. J. 5, 301-316 (1965)

Rall,W. : Membrane time constant of motoneurons. Science 126,454 (1957)

Rall,W. : Branching dendritic trees and motoneuron resistivity. Exp. Neurol. 1, 491-527 (1959)

Rall, W.: Membrane potential transients and membrane time constant of motoneurons. Exp. Neurol. 2, 503-532 (1960)

Rall, W. : Theory of physiological properties of dendrites. Ann. N.Y. Acad. Sci. 96, 1071-1092 (1962)

Redman, S.J., Lampard, D.G. : Monosynaptic stochastic stimulation of cat spinal motoneurons. I. Response of motoneurons to sustained stimulation. J. Neurophysiol. 31, 485-498 (1968)

Rinzel, J., Rall, W.: Transient response in a dendritic neuron model for current injected at one branch. Biophys. J. 14,759-790 (1974)

Roy, B.K., Smith, D.R. : Analysis of the exponential decay model of the neuron showing frequency threshold effects. Bull. Math. Biophys. 31, 341-357 (1969)

Stein, R.B. : A theoretical analysis of neuronal variability. Biophys. J. 5,173–194 (1965)

Stein, R.B. : Some models of neuronal variability. Biophys. J. 7, 38-68 (1967)

Tuckwell, H.C.: Determination of the interspike times of neurons receiving randomly arriving postsynaptic potentials. Biol. Cybern. 18, 225-237 (1975)

Tuckwell, H.C. : Synaptic transmission in a model for stochastic neural activity. J. Theor. Biol. 77, 65-81 (1979)

Tuckwell, H.C., Richter, W. : Neuronal interspike time distributions and the estimation of neurophysiological and neuroanatomical parameters. J. Theor. Biol. 71, 167-183 (1978)

Tuckwell, H.C., Wan, F.Y.M.: The response of a nerve cylinder to spatially distributed white noise inputs. J. Theor. Biol. 87, 275-295 (1980)

Vasudevan, R., Vittal, P.R. : Interspike interval density of the leaky integrator model neuron with a Pareto distributions of PSP amplitudes and with simulation of refractory time. J. Theor. Neurobiol. 1, 219-227 (1982)

Walsh, J.B. : A stochastic model of neuronal response. Adv. Appl. Prob. 13, 231-281 (1981)

Walsh, J.B., Tuckwell, H.C. : Determination of the electrical potential over dentritic trees by mapping onto a nerve cylinder. I.A.M.S. Tech. Report No. 83-9, Univ. British Columbia, Vancouver, BC, Canada (1983)

Wan, F.Y.M., Tuckwell, H.C. : The response of a spatially distributed neuron to white noise current injection. Biol. Cybern. 33, 39-55 (1979)

Wan, F.Y.M., Tuckwell, H.C. : Neuronal firing and input variability. J. Theor. Neurobiol. 1, 197-218 (1982)

Wan, F.Y.M., Wang, Y.S., Tuckwell, H.C. : First exit time for vector-valued diffusion processes and the neuronal firing time problem (1983) (to appear)

Wilbur, W.J., Rinzel, J. : A theoretical basis for large coefficient of variation and bimodality in neuronal interspike interval distributions (1983) (submitted)

White, B.C., Ellias, S. : A stochastic model for neuronal spike generation. SIAM J. Appl. Math. 37, 206-233 (1979)

Whitsel, B.L., Roppolo, J.R., Werner, G.: Cortical information processing of stimulus motion on primate skin. J. Neurophysiol. 35, 691-717 (1972)

Received: June 28, 1983

Prof. F. Y. M. Wan
Institute of Applied Mathematics and Statistics
University of British Columbia
Vancouver, BC, V6T1Y4
Canada